PHYSICAL REVIEW D **96,** 075022 (2017)

Constraints on top quark nonstandard interactions from Higgs boson and $t\bar{t}$ production cross sections

D. Barducci,[1] M. Fabbrichesi,[2] and A. Tonero[3]

[1]*SISSA and INFN, Sezione di Trieste, via Bonomea 265, 34136 Trieste, Italy*
[2]*INFN, Sezione di Trieste, Via Valerio 2, 34127 Trieste, Italy*
[3]*UNIFAL-MG, Rodovia José Aurélio Vilela 11999, 37715-400 Poços de Caldas, MG, Brazil*

(Received 27 April 2017; published 16 October 2017)

We identify the differential cross sections for $t\bar{t}$ production and the total cross section for Higgs production through gluon fusion as the processes in which the two effective operators describing the leading nonstandard interactions of the top quark with the gluon can be disentangled and studied in an independent fashion. Current data on the Higgs production and the $\mathrm{d}\sigma/\mathrm{d}p_T^t$ differential cross section provide limits comparable to, but not more stringent than, those from the total $t\bar{t}$ cross sections measurements at the LHC and Tevatron, where however the two operators enter on the same footing and can only be constrained together. We conclude by stating the (modest) reduction in the uncertainties necessary to provide more stringent limits by means of the Higgs production and $t\bar{t}$ differential cross section observables at the LHC with the future luminosity of 300 and 3000 fb^{-1}.

DOI: 10.1103/PhysRevD.96.075022

I. INTRODUCTION

The top quark is the heaviest among the standard model (SM) quarks and is therefore the best candidate to be studied for any departure from particle pointlike behavior. Such a departure would point to physics beyond the SM, possibly related to the dynamics behind the electroweak symmetry breaking (EWSB) mechanism.

The Large Hadron Collider (LHC) is expected to produce by the end of its run-3, with a collected integrated luminosity of 300 fb^{-1}, roughly 2×10^8 top quark pairs, effectively acting as a *top factory* and thus providing the possibility of scrutinizing the top quark intrinsic properties with an unprecedented precision. Moreover, the top quark enters in the dominant Higgs production mechanism at the LHC, the production via gluon fusion, which is also expected to be measured with high accuracy by the end of the LHC program.

The study of the properties of the top quark has been performed both in terms of anomalous couplings [1–7] and of SM higher dimensional effective operators [8–15], often with an overlap between the two approaches. While the anomalous-coupling approach has the advantage of a more direct physical interpretation and the lower number of parameters, the effective Lagrangian framework provides a more general and unbiased view, based on the possibility of performing global fits on a larger number of operators affecting various processes; see e.g. [16,17].

In this work, motivated by the fact that strong interactions dominate $t\bar{t}$ production at the LHC, we follow the anomalous coupling approach, by studying the top-quark hypothetical structure only by means of its interaction to gluons. We parametrize it in terms of the following $SU(3)_C \times U(1)_{em}$ effective operators,

$$\mathcal{O}_1 = \frac{C_1}{\Lambda^2}\bar{t}\gamma^\mu T^a t D^\nu G^a_{\mu\nu} \tag{1}$$

$$\mathcal{O}_2 = \frac{C_2}{\Lambda^2} v \bar{t}\sigma^{\mu\nu} T^a t G^a_{\mu\nu}, \tag{2}$$

where $T^a = \lambda^a/2$ are the $SU(3)_C$ generators; $[T^a, T^b] = i f_{abc} T^c$ and $\mathrm{Tr}[\lambda^a \lambda^b] = 2\delta^{ab}$; $D^\nu = \partial^\nu - i g_s G^{\nu,a} T^a$ and $G^a_{\mu\nu} = \partial_\mu G^a_\nu - \partial_\nu G^a_\mu + g_s f^{abc} G^b_\mu G^c_\nu$ are the $SU(3)_C$ covariant derivative and the field strength tensor respectively; and $\sigma^{\mu\nu} = i/2[\gamma^\mu, \gamma^\nu]$. These two effective operators can also be seen as the leading terms coming from the Taylor expansion of the strong version of the Dirac and Pauli form factors in the top gluon interaction [18], thus making perhaps more evident the relationship with the study of the internal structure of the top quark. This point will be discussed in Sec. I A. The vacuum expectation value $v = 174$ GeV in Eq. (2) is a reminder of the presence of the Higgs boson in the $SU(2)_L$ invariant operator before EWSB. This will induce further interactions affecting Higgs phenomenology which we will discuss in Sec. III.

The effective operators of Eqs. (1) and (2) affect both $t\bar{t}$ and Higgs production processes, which can then be used to constrain the corresponding Wilson coefficients. The relation between the operator $\mathcal{O}_1$ of Eq. (1) and the four-fermion operators in the Warsaw basis [19] is given in the Appendix. Because of its space-time structure, the three-point function arising from the operator $\mathcal{O}_1$ vanishes when coupled to on-shell gluons, and thus does not affect the dominant Higgs production mechanism at the LHC, the one via gluon fusion, which can then be used to constrain the size of the operator $\mathcal{O}_2$ independently of $\mathcal{O}_1$. On the other hand, even though the operator $\mathcal{O}_2$ enters both processes, its contribution only marginally modifies the shape of the

top quark pair invariant mass and transverse momentum distributions [20]. Modifications are present in the high energy regime when quadratic terms in C_2 are retained. Therefore for small values of the Wilson coefficient negligible departures with respect to the SM predictions are expected. In order words, the shapes of the normalized $1/\sigma \mathrm{d}\sigma/\mathrm{d}m_{t\bar{t}}$ and $1/\sigma \mathrm{d}\sigma/\mathrm{d}p_T^t$ distributions are essentially unaffected by the presence of the $\mathcal{O}_2$ operator.

We thus conclude that the combined study of the inclusive Higgs production and of the differential cross sections for $t\bar{t}$ production could offer two observables constraining the operators $\mathcal{O}_1$ and $\mathcal{O}_2$ independently of each other, thus providing, in principle, more stringent limits than those we can obtain from other processes, like the total cross section, where the simultaneous presence of both operators requires some marginalization in order to set the constraints.

As we will show, the use of these independent observables to set more stringent limits is only possible if the uncertainties in the differential cross section measurements can be reduced, especially in the high momentum-transfer region. While this is expected to happen as more data will be collected, it is not the case yet for those currently available. For this reason we still use the total $t\bar{t}$ production cross section—where both $\mathcal{O}_1$ and $\mathcal{O}_2$ enter—to set the strongest limits available today. We then identify the expected reduction in uncertainty necessary to have the $t\bar{t}$ differential cross section and Higgs production process to set the most stringent limit on the operator $\mathcal{O}_1$ independently of $\mathcal{O}_2$ at the LHC with the future luminosity of 300 and 3000 fb^{-1}.

A. Form factors and gauge invariance

The physical interpretation of the contribution of the operators in Eqs. (1) and (2) to cross section measurements is in terms of a departure from the pointlike behavior of the top quark. From this point of view, as already mentioned in the previous section, these operators can be seen as the leading terms coming from the Taylor expansion of the strong version of the electromagnetic form factors.

In order to explain this point, it is useful to first recall how nucleon electromagnetic form factors are defined. They are usually introduced through an effective parametrization of the nucleon-photon vertex Γ_μ which in momentum space reads as follows:

$$\Gamma_\mu(q,k) = e\gamma_\mu F_1(q^2) + ie\frac{\sigma_{\mu\nu}}{2M}q^\nu F_2(q^2), \tag{3}$$

where q is the photon momentum and F_1 and F_2 are. respectively, the Dirac and Pauli form factors, with $F_1(0) = 1$ and $F_2(0) = \kappa$. This parametrization of the vertex respects electromagnetic gauge invariance when considering on-shell external nucleons.

In the case of strong interactions, where the underlying $SU(3)_C$ symmetry is non-Abelian, a parametrization similar to that of Eq. (3) would violate gauge invariance. Therefore, form factors that respect gauge invariance have to be introduced by considering, in addition to the covariant kinetic term, the following operators:

$$\bar{\psi}\left[\frac{C_1}{\Lambda^2}\gamma^\mu f_1\left(\frac{D^2}{\Lambda^2}\right)D^\nu G_{\mu\nu} + \frac{C_2}{\Lambda}\sigma^{\mu\nu} f_2\left(\frac{D^2}{\Lambda^2}\right)G_{\mu\nu}\right]\psi, \tag{4}$$

where $D^2 = D_\mu D^\mu$. The functions f_1 and f_2 are the strong analogues of the Dirac and Pauli form factors. These form factors are assumed to admit a Taylor expansion. The leading terms of the expansion are what we consider in our study and are represented by the operators introduced in Eqs. (1) and (2).

While in the case of electromagnetic interactions, form factors can be introduced in a way that their presence affects just the interaction vertex between one single photon and the fermion, in the case of strong interactions, gauge invariance requires that form factors affect also interaction vertices between the fermion and multiple gluons. This can be seen by expanding the functions f_1 and f_2 in Eq. (4) and substituting the explicit expression of the covariant derivative.

B. The fine print

The reliability of the perturbative expansion of the effective theory depends on the relative size of the higher order operators with respect to those we retain in the cross section. This size is controlled by the energy of the process, the energy scale of the effective theory and the estimated strength of couplings. Regarding the leading corrections to the SM result, the size of which is controlled by g_{SM}, and indicating with $\bar{E}$ the energy probed in the process, we have the terms

$$O\left(\frac{g_{\mathrm{SM}}C^{(6)}\bar{E}^2}{\Lambda^2}\right), \tag{5}$$

which arise from the interference between the SM amplitude and the leading dimension-six operators, the terms

$$O\left(\frac{C^{(6)}\bar{E}^2}{\Lambda^2}\right)^2, \tag{6}$$

which come from the square (or the double insertion) of the same dimension-six operators, and the terms

$$O\left(\frac{g_{\mathrm{SM}}C^{(8)}\bar{E}^4}{\Lambda^4}\right), \tag{7}$$

which originate from the interference between the SM amplitude and the dimension-eight operators.

The terms in Eq. (7) are formally comparable to those in Eq. (6). Without any assumption about the strength of the interactions behind the effective operators, it is not possible to decide whether the terms in Eq. (7) should be included or can be safely neglected. To make such an assumption manifest we can rewrite the coefficients $C^{(6)}$ and $C^{(8)}$ as $g_\star \tilde{C}^{(6)}$ and $g_\star \tilde{C}^{(8)}$, where $g_\star$ indicates the strength of these interactions. Accordingly, the condition for the terms in Eq. (7) to be smaller than those in Eq. (6) is simply

$$g_\star > g_{\mathrm{SM}}. \tag{8}$$

In our study, we look into departures from pointlike behavior of the top quark. It is then reasonable to assume that such physics originates in interactions that are at least stronger than those of the standard model. This assumption makes the condition in Eq. (8) satisfied. This argument must be taken with a grain of salt: it is an assumption that $C^{(8)} = g_\star \tilde{C}^{(8)}$, rather than higher powers of $g_\star$, and it is another assumption that the numerical coefficients are sufficiently small for making dimensional analysis valid.

When the terms in Eq. (5) are larger than the SM result itself, it is necessary to include also those in Eq. (6) in order to make a likelihood test well defined (this point was already made in [21]). The reason is that otherwise the observable to be estimated could be negative for negative values of the coefficient $C^{(6)}$. This can happen if the energy $\bar{E}$ in the process is large enough to overcome in Eq. (5) the suppression from $O(g_{\mathrm{SM}} C^{(6)}/\Lambda^2)$. This is the case in our estimate of the total and differential cross sections because $\bar{E} = m_{t\bar{t}}$ (where $m_{t\bar{t}}$ is the invariant mass of the system of top quark pairs) can become large enough. We therefore must include the terms in Eq. (6). On the other hand, the cross section for the Higgs boson production is safe because $\bar{E} = m_H$ (where m_H is the mass of the Higgs boson) and we can keep only terms of the type of Eq. (5).

Another comment is in order. Next-to-leading order (NLO) corrections to the processes under consideration are crucial in order to match the theoretical predictions with the experimental measurements. It is therefore in principle necessary to evaluate all amplitudes at least to this order, both for the SM and in the case of the presence of the operators $\mathcal{O}_1$ and $\mathcal{O}_2$ of Eqs. (1) and (2). It has however been recently shown [20] that these corrections, at least regarding the operator $\mathcal{O}_2$, only affect the cross section by an overall k-factor which is equal for the SM and for the SM augmented by the operator $\mathcal{O}_2$. This holds true both for the total cross section, as well for the differential ones, where the k-factors are now approximately equal to each other bin per bin. Pending a formal proof, we will assume that the same holds true also for the operator $\mathcal{O}_1$. For this reason, we perform our calculation at the leading order (LO).

II. TOP PAIR PRODUCTION CROSS SECTION MEASUREMENTS

In order to calculate total and differential event rates for the $t\bar{t}$ process, we implement the operators of Eqs. (1) and (2) in the `UFO` [22] format through the `Feynrules` [23] package and use `MadGraph5_aMC@NLO` [24] as an event generator. We then analyze the generated event via the `MadAnalysis5` [25] package.

We perform our calculation at the leading order and in comparing our results with the $t\bar{t}$ rates (both total and differential) we assume that the central value of the experimental measurement corresponds to the SM predicted cross section, computed by fixing $C_1 = C_2 = 0$ in our numerical calculation. In other words, we are computing *expected limits* on the two Wilson coefficients, as it is usually done when calculating limits for projected measurements. In the case of actual data, we are assuming that the mismatch between the measured values and the SM predictions, when folded with the relevant k factors, is due to the statistical fluctuation that we ignore.

A. Limits from the total cross section

The contribution of the two operators in Eqs. (1) and (2) to the total cross section for $t\bar{t}$ production has been previously estimated and limits on their size obtained. The most recent analysis of the two operators taken by themselves can be found in [18], while one considering the full set of operators affecting top quark phenomenology has been presented in [16] by the use of the dedicated package `TopFitter`.

We update here these constraints by means of the most precise 13 TeV LHC data. The CMS Collaboration recently released a measurement of the top quark pair total cross section performed in the single lepton channel with an integrated luminosity of 3.2 fb^{-1} [26]. This measurement yields a value for the total cross section of

$$\sigma(pp \to t\bar{t}) = 835 \pm 3(\mathrm{stat}) \pm 23(\mathrm{syst}) \pm 23(\mathrm{lum})\ \mathrm{pb}. \tag{9}$$

The relative error on this measurement, after having summed in quadrature the various sources of uncertainty, is about 3.9%, comparable to the one obtained with the combination of 7 and 8 TeV data in the dileptonic channel [27].

The operator of Eq. (1) does not affect the partonic process $gg \to t\bar{t}$, thus only modifying the $q\bar{q}$ initiated reaction, which at the LHC is subdominant in the $t\bar{t}$ cross section, given that the antiquark parton has to be extracted from the sea quarks of the proton. This comes about because of gauge invariance and the presence of a contact vertex with two gluons attached to the quark lines [see Fig. 1(a) and (c)], a contribution which cancels out that of the vertex with a single gluon. For this reason the Wilson coefficient C_1 can be more effectively constrained by Tevatron data, where the antiquark state is extracted from

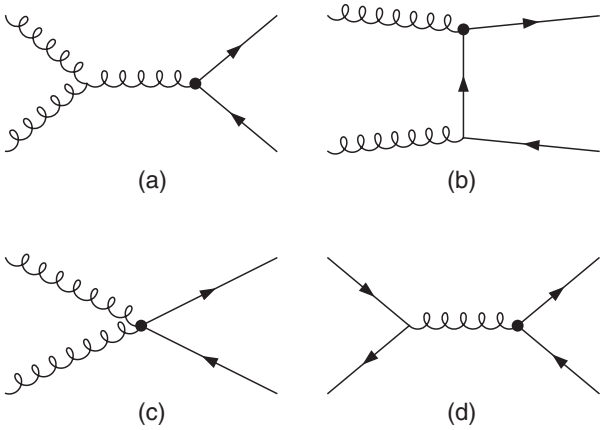

FIG. 1. Representative Feynman diagrams for $t\bar{t}$ production through gluon fusion (a)–(c) and quark-antiquark annihilation (d). The black dots represent the insertion of one of the two operators of Eqs. (1) and (2).

the valence quarks of the colliding antiproton. A combined result from the CDF and D0 collaborations gives the following measurement of the total $t\bar{t}$ cross section [28],

$$\sigma(p\bar{p} \to t\bar{t}) = 7.65 \pm 0.42 \text{ pb}, \tag{10}$$

with a relative precision of about 5.5%, which we use throughout our analysis.

Following the procedure described at the beginning of this section, and by fixing one of the two Wilson coefficients to zero, we obtain the limits from the total $t\bar{t}$ cross section measurements which are shown in Fig. 2, where the blue and green shaded areas correspond to the 95% confidence level uncertainties on the cross section determination at the LHC and Tevatron respectively, and the solid lines correspond to the relative modification of the SM cross section due to the presence of the operators $\mathcal{O}_1$ and $\mathcal{O}_2$. If we allow for the presence of both operators at the same time, we obtain the limits shown in Fig. 3. The two exclusion regions have different inclinations because the operator $\mathcal{O}_1$ contribution depends on the different relative importance of the gluon and quark initiated reaction at the Tevatron and the LHC. The importance of the Tevatron data in constraining the C_1 Wilson coefficient is thus manifest, the bound being a factor 3 better for $C_1 > 0$ (taking $C_2 = 0$).

B. Limits from the differential cross sections

The current center of mass energy for LHC proton collisions, as well as the large number of top quark pairs expected to be produced during the present run of the CERN machine, will allow us to measure top quark differential cross sections with an unprecedented precision and with a potentially large number of events populating the tails of such distributions, thus allowing for a more stringent comparison between experimental measurements and theoretical predictions. In fact, other than modifying the total rate for $t\bar{t}$ production, the effective operators in

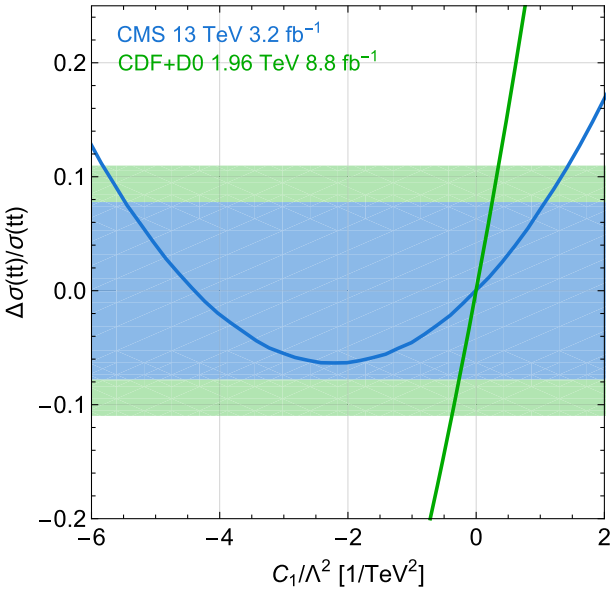

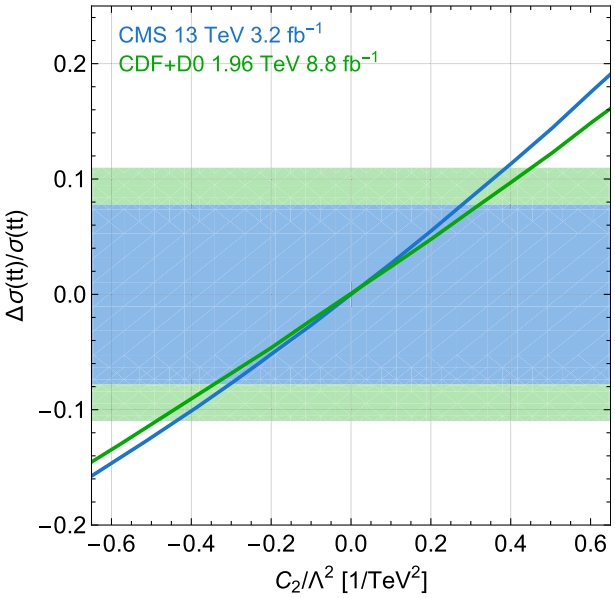

FIG. 2. Relative modification of the $t\bar{t}$ total cross section, $\Delta\sigma(t\bar{t})/\sigma(t\bar{t}) = \sigma(t\bar{t})^{\text{BSM}}/\sigma(t\bar{t})^{\text{SM}} - 1$, induced by the presence of the operators $\mathcal{O}_1$ and $\mathcal{O}_2$. The blue and green shaded regions correspond to the 95% confidence level intervals on the Wilson coefficients C_1 and C_2 from the cross section determination from LHC and Tevatron data respectively. The limits can be found by looking at the intersections of the curves with the regions of the same color: $-5.48/\text{TeV}^2 < C_1 < 1.08/\text{TeV}^2$ and $-0.30/\text{TeV}^2 < C_2 < 0.28/\text{TeV}^2$ for the LHC and $-0.38/\text{TeV}^2 < C_1 < 0.35/\text{TeV}^2$ and $-0.49/\text{TeV}^2 < C_2 < 0.45/\text{TeV}^2$ for the Tevatron.

Eqs. (1) and (2) can in principle affect the shape of the cross sections' differential distributions, altering them with respect to the SM predictions. Therefore the possibility of using *differential measurements* other than total cross sections potentially offers a powerful means to constrain the coefficients of these higher dimensional operators.

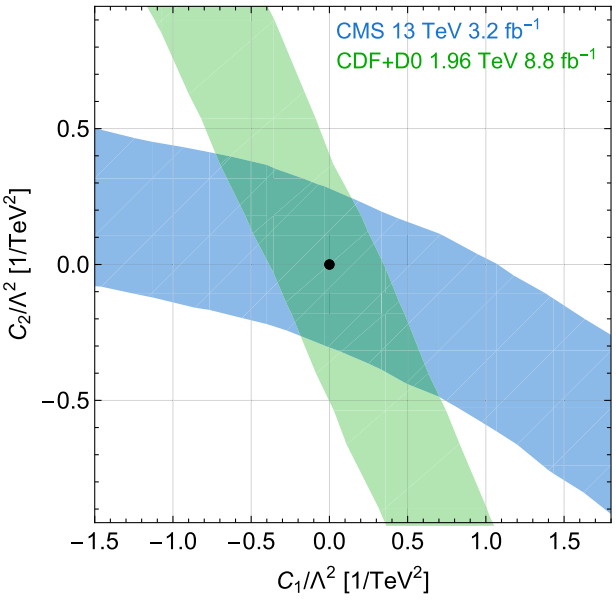

FIG. 3. 95% confidence intervals on the Wilson coefficients C_1 and C_2 from the measurements of the $t\bar{t}$ total cross section at the LHC (blue) and Tevatron (green). The corresponding combined limits are listed in Table II.

In particular, both the top quark pair invariant mass differential distribution ($\mathrm{d}\sigma/\mathrm{d}m_{t\bar{t}}$) and the top quark transverse momentum differential distribution ($\mathrm{d}\sigma/\mathrm{d}p_T^t$) present interesting behavior with respect to the two operators of Eqs. (1) and (2). The insertion of the $\mathcal{O}_1$ operator gives rise to the typical tail enhancement in the distributions at large invariant masses and transverse momentum, as shown in Fig. 4, where the differential rates normalized to the total cross section are computed for both the case of the top pair invariant mass distribution and top quark transverse momentum.

On the other hand, for high invariant masses and transverse momenta, the shapes of the differential distributions computed in the presence of the operator $\mathcal{O}_2$ are not modified with respect to the SM when just the linear order in the Wilson coefficient C_2 is retained. This is true at LO [9] but also at NLO, as shown in [20], where both the SM and the EFT contributions are evaluated at NLO order. The computation of [20] shows that evaluating both terms at NLO order avoids an overestimation of the enhancement of the contribution of the $\mathcal{O}_2$ operator in the high energy regime.

The inclusion of quadratic terms in C_2 modifies the high energy tails of the distributions already at tree level. In [29], the authors retain up to quartic terms in the effective operator coefficients for computing the cross sections and find an enhancement of the sensitivity in the ultraboosted regime. However, the contribution of these quadratic terms is negligible if the specific values of C_2 used to generate the distributions in the relevant energy range are sufficiently small (see Fig. 4).

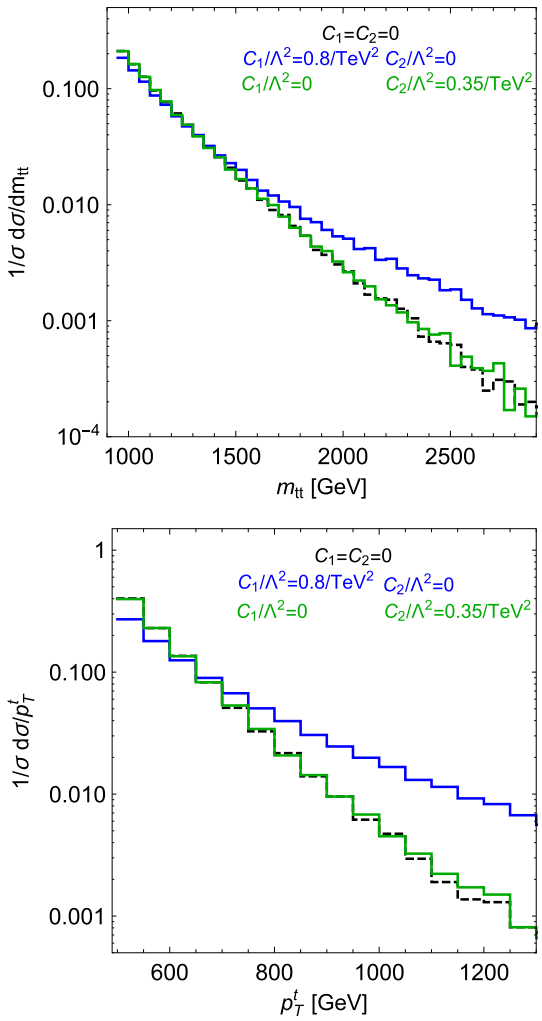

FIG. 4. Differential distribution for top quark pair production with respect to the top pair invariant mass and the top transverse momentum normalized to unity for the case where just the operator $\mathcal{O}_1$ is inserted (solid blue) and just the operator $\mathcal{O}_2$ is inserted (solid green). The SM prediction is shown in dashed black. The relative independence from $\mathcal{O}_2$ is manifest. Also, it is for large $m_{t\bar{t}}$ and p_T^t that the distributions are most sensitive to the insertion of $\mathcal{O}_1$.

Regarding our analysis, the different behaviors of the two operators suggest that the *normalized* differential cross section measurements can be used to set a limit on the coefficient of the $\mathcal{O}_1$ operator, irrespective of the value taken by the $\mathcal{O}_2$ operator.

From the experimental side, while the invariant mass distribution of the top quark pairs, $m_{t\bar{t}}$, has been previously measured by both the CDF and D0 collaborations at Tevatron [30,31], more recently both the ATLAS and CMS collaborations have provided unfolded measurements of this and others observable both normalized to the total event rate and to unity [32–36]. We will use the ATLAS differential measurements of [35] which have been performed in the all hadronic channel with an integrated

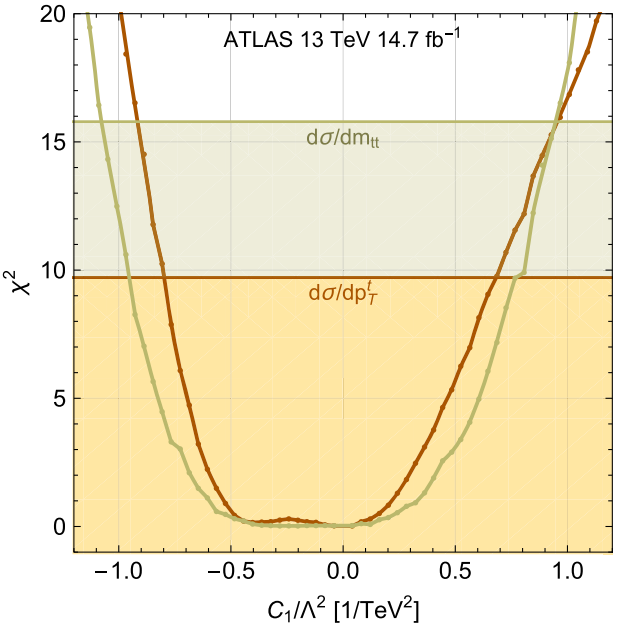

FIG. 5. χ^2 distribution for the Wilson coefficient C_1 from the differential cross section measurement in $t\bar{t}$ invariant mass and top quark transverse momentum of [36]. The horizontal lines represent the 95% confidence level limit taken for a χ^2 with 8 degrees of freedom corresponding to the 9 bins of data considered in the $1/\sigma \mathrm{d}\sigma/\mathrm{d}m_{t\bar{t}}$ distribution and 5 degrees of freedom corresponding to the 6 bins of data considered in the $1/\sigma \mathrm{d}\sigma/\mathrm{d}p_T^t$ distribution.

luminosity of 14.7 fb^{-1}, exploiting a final state with a highly boosted top, which has been shown to be effective in testing the top quark intrinsic structure [29].

We thus perform a χ^2 fit to the measured top quark normalized invariant mass and transverse momentum distributions (see Fig. 5), again assuming that the central value of the experimental measurements coincides with our predictions when $C_1 = C_2 = 0$, with the uncertainties reported in Table I. The number of degrees of freedom for the χ^2 fit correspond to the number of bins of the considered distribution minus 1, since one degree of freedom is fixed by the requirement that the area under the curve is equal to unity. With this procedure, and taking the data for the p_T^t distribution which turn out to provide the most stringent constraint, we set a limit of $-0.80/\mathrm{TeV}^2 < C_1/\Lambda^2 < 0.68/\mathrm{TeV}^2$, which is comparable with the one that can be obtained through the total cross section measurements. We will show in Sec. IV the prospects for the determination of the C_1 coefficient with the increase of the data collected by the LHC.

TABLE I. Top pair invariant mass and top quark transverse momentum binning of the ATLAS measurements of the $t\bar{t}$ invariant mass differential cross section and relative errors in percent [35]. The observable values indicate the lower edge of the considered bin except for the last bin where the upper values are explicitly indicated.

$m_{t\bar{t}}$ (TeV)	1.0	1.1	1.2	1.3	1.4	1.5	1.7	2.0	2.3–3.0
Error (%)	36	20	25	30	31	32	63	58	123

p_T^t (TeV)	0.5	0.55	0.6	0.65	0.75	0.9–1.2
Error (%)	19	25	28	45	73	95

III. HIGGS PRODUCTION CROSS SECTION MEASUREMENTS

The production of the Higgs boson at the LHC is dominated by the gluon fusion channel. This process arises in the SM from a one-loop diagram mediated by colored fermions, the amplitude being dominated by the top quark contribution because of its large Yukawa coupling to the Higgs boson. It has been discussed as an observable sensitive to the operator $\mathcal{O}_2$ in [11,37].

The presence of the higher dimensional operators of Eqs. (1) and (2) introduces modifications to the coupling between the top quark and the gluon, thus affecting the Higgs boson production rate. Only the $\mathcal{O}_2$ operator contributes to this process because for on-shell gluons the correction arising from $\mathcal{O}_1$ identically vanishes. This is obvious if one recalls that the operator $\mathcal{O}_1$ can be written in terms of four-fermion operators, as shown in the Appendix. Therefore the amplitude for $gg \to H$ can be written as the sum of two contributions

$$\mathcal{M} = \mathcal{M}_{\mathrm{SM}} + \mathcal{M}_{\mathcal{O}_2}, \tag{11}$$

where $\mathcal{M}_{\mathrm{SM}}$ is the SM contribution and $\mathcal{M}_{\mathcal{O}_2}$ is the contribution coming from one insertion of the $\mathcal{O}_2$ operator. Terms coming from two insertions of the dipole operator are neglected, since in the end we are going to retain only contributions linear in C_2, as discussed in Sec. I B. We assume that the Yukawa coupling between the top quark and the Higgs boson takes its SM value and we take a zero finite contribution from the operator $\mathcal{O}_{HG} = H^\dagger H G^a_{\mu\nu} G_a^{\mu\nu}$. Furthermore we assume that their mixing with the operators of Eqs. (1) and (2) is negligible. With these assumptions we can use the $gg \to H$ process to set a direct limit on the coefficient of the $\mathcal{O}_2$ operator. We rewrite the effective operator of Eq. (2) in its $SU(2)_L \times U(1)_Y$ invariant form in order to correctly take into account all the contributions affecting Higgs phenomenology arising from the operator $\mathcal{O}_2$; see Fig. 6.

We compute the Higgs production cross section analytically, cross-checking the results by means of `Package X` [38]. The final numerical integration of the Feynman integrals has also been checked against `FormCalc8` [39]. A factor 4 takes into account the identical contributions coming from crossing the gluon lines and switching the vertex insertion of the dipole operator. The contribution of Fig. 6(b) turns out to be identically zero in dimensional regularization. We therefore have

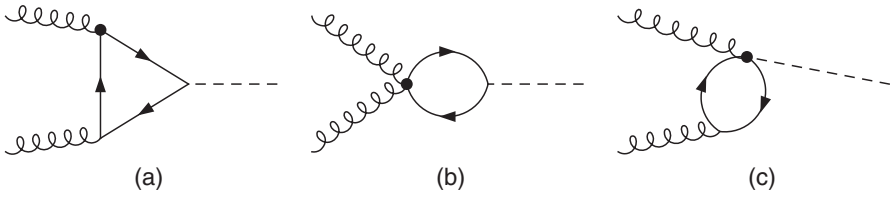

FIG. 6. Representative Feynman diagrams (a) and (b) for Higgs boson production through gluon fusion. The black dots represent the insertion of the operator of Eq. (2).

$$(\mathcal{M}_{\mathcal{O}_2})^{ab}_{\lambda_1\lambda_2} = 4\times g_s \frac{m_t}{\sqrt{2}}\frac{2C_2}{\Lambda^2}\frac{1}{16\pi^2}(m_H^2 g_{\mu\nu} - 2q_{2\mu}q_{1\nu})\varepsilon^{\mu}_{\lambda_1}(q_1)\varepsilon^{\nu}_{\lambda_2}(q_2)\mathrm{Tr}[T^a T^b]\times\left\{\frac{1}{\bar{\epsilon}} + 1 - \log\frac{\mu^2}{m_t^2}\right.$$
$$\left. + \frac{m_t^2}{m_H^2}\log^2\left(\frac{\sqrt{m_H^4 - 4m_t^2 m_H^2} + 2m_t^2 - m_H^2}{2m_t^2}\right) + \frac{\sqrt{m_H^4 - 4m_t^2 m_H^2}}{m_H^2}\log\left(\frac{\sqrt{m_H^4 - 4m_t^2 m_H^2} + 2m_t^2 - m_H^2}{2m_t^2}\right)\right\} \quad (12)$$

where m_t and m_H are the masses of the top quark and the Higgs boson. The vectors $\varepsilon^{\mu}_{\lambda_1}(q_1)$ and $\varepsilon^{\nu}_{\lambda_2}(q_2)$ represent the polarizations for the two incoming gluons with momenta q_1 and q_2. We regularize the divergent loop integral by means of dimensional regularization where the pole in four dimensions is written in the $\overline{\mathrm{MS}}$ scheme, i.e. $1/\bar{\epsilon} = 1/\epsilon - \gamma_E + \log(4\pi)$.

In order to have a finite amplitude we subtract the $1/\bar{\epsilon}$ pole by a counterterm proportional to the effective operator describing the direct coupling of the Higgs boson to the gluon fields: $\mathcal{O}_{HG} = H^\dagger H G^a_{\mu\nu} G_a^{\mu\nu}$. This renormalization procedure leaves a logarithmic dependence on the subtraction scale, for which we take $\mu = m_H$ to match the factorization scale for the process. We also explicitly checked that indeed the double insertion of the $\mathcal{O}_2$ operator gives rise to a small correction that can be neglected, as discussed in Sec. I B.

In computing the squared amplitude of Eq. (11) the leading correction to the SM cross section is a term linear in the C_2 Wilson coefficient. By fixing $m_t = 172$ GeV and $m_H = 125$ GeV we find that the ratio of the gluon fusion Higgs production cross section with respect to its SM value is

$$\mu_{\mathcal{O}_2} \simeq 1 + 0.375\ \mathrm{TeV}^2\frac{C_2}{\Lambda^2}. \quad (13)$$

This ratio is measured experimentally and usually presented by the experimental collaborations either in terms of signal strength values, which is precisely the ratio of the experimental measurements with respect to the SM expectation, or of the coupling modifier, the ratio of the Higgs to gluon gluon effective coupling compared with the SM prediction. In either case, the results of Eq. (13) allow us to directly use the current precision on the Higgs production measurements and set a limit on the C_2 Wilson coefficient.

As for the computation of the $t\bar{t}$ production cross section, this ratio has been obtained at LO. We however assume these results to hold also at NLO since the k factor induced by higher order corrections is expected to be the same for the SM and the effective operator cases, therefore canceling out in performing the ratio.

The ATLAS and CMS collaborations have performed a combined measurements of the Higgs signal strength with about 5 and 20 fb^{-1} of data collected during the 7 and 8 TeV run of the LHC, yielding a value for the gluon fusion Higgs production signal strength [40]

$$\mu_{ggH} = 1.03^{+0.17}_{-0.15}. \quad (14)$$

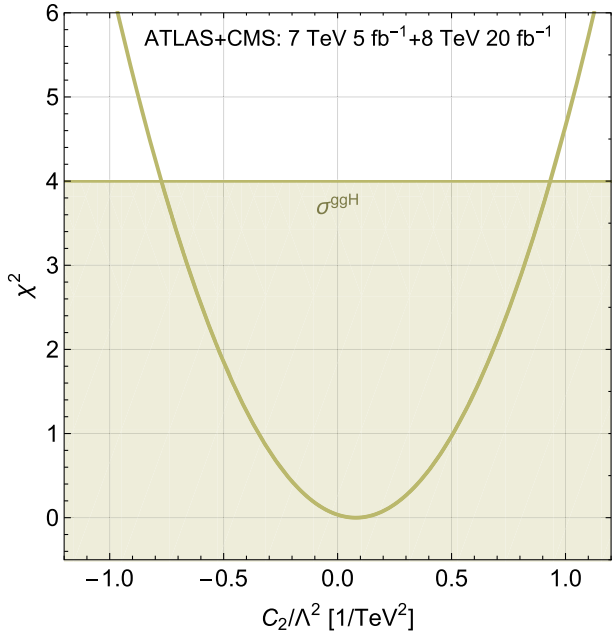

FIG. 7. χ^2 distribution for the Wilson coefficient C_2 from the Higgs production from gluon fusion. The horizontal line represents the 95% confidence level limit taken for a χ^2 with one degree of freedom.

TABLE II. Limits at 95% confidence level on the coefficients C_1 and C_2 from current data. Values in the first column come from the total cross sections and are obtained by marginalization of one operator against the other. The limits in the next two columns are obtained for the two operators independently by means of Higgs production and the indicated differential cross section. All values are in units of TeV^{-2}.

$\sigma_{t\bar{t}}$ (Tevatron + LHC)	μ_{ggH}	$\mathrm{d}\sigma_{t\bar{t}}/\mathrm{d}p_T^t$
$-0.74 < C_1/\Lambda^2 < 0.71$	⋯	$-0.80 < C_1/\Lambda^2 < 0.68$
$-0.49 < C_2/\Lambda^2 < 0.42$	$-0.77 < C_2/\Lambda^2 < 0.93$	⋯

The χ^2 value for the parameter C_2 is shown in Fig. 7, from which we find the 95% confidence level limits $-0.77/\mathrm{TeV}^2 < C_2/\Lambda^2 < 0.93/\mathrm{TeV}^2$, also reported in Table II. This estimate provides limits on the coefficient of the $\mathcal{O}_2$ operator, which are not yet competitive with those obtained from the measurements of the top pair production cross section. We will show in the next section how the expected improvement on the determination of this signal strength will provide stronger limits on the C_2 Wilson coefficient.

IV. COMBINATION AND PROSPECTS

In the previous sections we have shown that the measurement of the normalized top quark transverse momentum differential distribution in top pair production and the measurement of the Higgs boson production cross section through gluon fusion can be used to set *independent limits* on the coefficient of the operators $\mathcal{O}_1$ and $\mathcal{O}_2$ respectively. We show in Fig. 8 the limits on the C_1 and C_2 Wilson coefficient obtained through this method, together with those obtained only by means of the measurements of the total top pair production cross sections performed at both the Tevatron and LHC. Table II summarizes the various bounds. These bounds are the most stringent among those so far available for the operators $\mathcal{O}_1$ and $\mathcal{O}_2$ (compare with those in [16,18]).

The proposed method thus sets limits comparable to those obtained from total $t\bar{t}$ cross section measurements on the operator $\mathcal{O}_1$ and roughly a factor two weaker on the operator O_2. However, while the current uncertainties on the measurement of the top quark pair total cross section, which are about 4%, are not going to improve substantially, this is not the case for the top quark differential cross sections as well as for the Higgs production cross section measurements which are expected to become more precise. In order to infer the projected limits on the C_1 and C_2 Wilson coefficients we thus proceed in the following way.

For the measurements of the top quark transverse momentum differential cross section we rescale the uncertainties reported in Table I by the luminosity dependent factor $\sqrt{\mathcal{L}_0/\mathcal{L}}$ where $\mathcal{L}_0 = 14.7\ \mathrm{fb}^{-1}$ indicates the current collected luminosity and $\mathcal{L}$ the projected luminosity. We finally take the error associated with this measurement to be

$$\left.\frac{\Delta\sigma}{\sigma}\right|_{\mathcal{L}} = \mathrm{Max}\left[0.15, \left.\frac{\Delta\sigma}{\sigma}\right|_{\mathcal{L}_0} \times \sqrt{\frac{\mathcal{L}_0}{\mathcal{L}}}\right], \tag{15}$$

thus assuming a conservative floor of 15% for the error estimation.

For the Higgs production through gluon fusion process, we use the projected uncertainties on the measurements as provided by the CMS Collaboration [41] which are 5.7% (2.7%) for a collected integrated luminosity of 300 (3000) fb^{-1}.

Through this procedure we obtain the expected limits on the Wilson coefficients C_1 and C_2 shown in Fig. 9 where the light and dark gray regions correspond to integrated luminosities of 300 and 3000 fb^{-1} respectively. For comparison, the previous limits obtained from the measurements of the total $t\bar{t}$ cross section at the Tevatron and LHC are also shown.

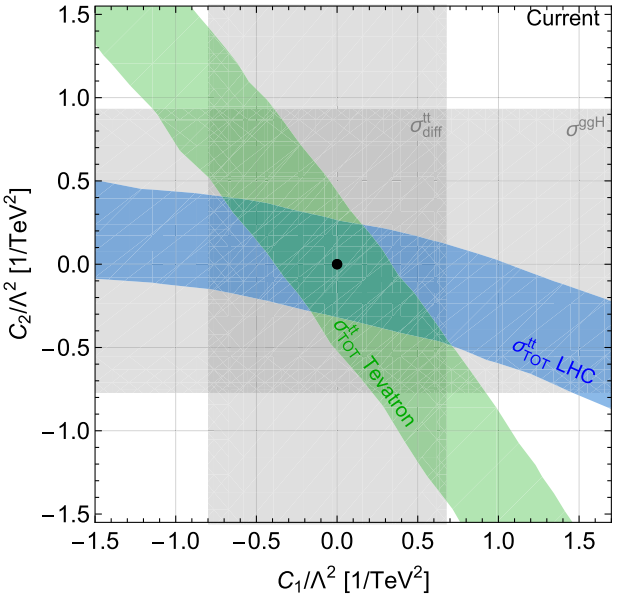

FIG. 8. 95% confidence intervals for C_1 and C_2 from the measurements of the top quark transverse momentum differential cross section and Higgs production via gluon fusion cross section (vertical gray and horizontal gray shaded area respectively), with current available data. The limits from the measurements of $t\bar{t}$ total cross section at the LHC (blue) and Tevatron (green) are also shown.

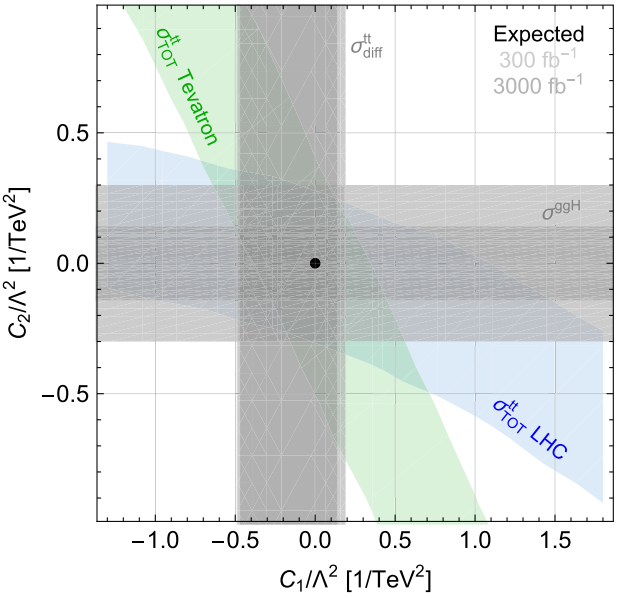

FIG. 9. 95% confidence intervals for C_1 and C_2 from the measurements of the top quark transverse momentum differential cross section and Higgs production via gluon fusion cross section (vertical gray and horizontal gray shaded area respectively). The lighter (darker) gray area corresponds to an integrated luminosity of 300 (3000) fb^{-1} respectively. The limits from the measurements of the $t\bar{t}$ total cross section at the LHC (blue) and Tevatron (green) are also shown.

The plot shows that with an integrated luminosity of 300 fb^{-1} the combination of the differential measurements in $t\bar{t}$ production together with the measurements of the Higgs production rate through gluon fusion will be able to set a comparable limit on the C_2 Wilson coefficient, and a stronger limit on C_1 for $C_1 > 0$. At the end of the LHC program, that is, with an integrated luminosity of 3000 fb^{-1}, these measurements will provide the most stringent limits on the coefficient of the $\mathcal{O}_1$ and $\mathcal{O}_2$ operators. We report these values in Table III. All the limits can be turned around to be reexpressed as lower bounds on Λ, the scale of the effective theory, by fixing $C_1 = C_2 = 4\pi$ and taking the absolute value of the limits in Table II. Accordingly we find

$$\Lambda \gtrsim 4.3 \text{ TeV} \quad \text{and} \quad \Lambda \gtrsim 5.5 \text{ TeV} \tag{16}$$

from, respectively, the operator in Eqs. (1) and (2). The reliability of the expansion in the effective field theory approach is verified if the probed energies $\bar{E} < \Lambda$. This is true for the Higgs production. It holds for the differential top pair production measurement analysis as well, even though in this case, as the explored transferred energies go up to about 3 TeV, we are approaching the limit. The bounds of Eq. (16) could be raised to almost 9 TeV with the expected reduced uncertainties.

TABLE III. Expected limits at 95% confidence level on the coefficients C_1 and C_2 from future data from $d\sigma_{t\bar{t}}/dp_T^t$ and μ_{ggH} respectively. Values are in units of TeV^{-2}.

LHC 300 fb^{-1}	LHC 3000 fb^{-1}
$-0.49 < C_1/\Lambda^2 < 0.19$	$-0.47 < C_1/\Lambda^2 < 0.19$
$-0.30 < C_2/\Lambda^2 < 0.30$	$-0.14 < C_2/\Lambda^2 < 0.14$

ACKNOWLEDGMENTS

We thank Marina Cobal and Michele Pinamonti for discussions. M. F. is associated with SISSA and the Department of Physics, University of Trieste. The work of A. T. is supported by Coordenação de Aperfeiçoamento de Pessoal de Nível Superior (CAPES). A. T. would like to thank T. Hahn for the help with `FormCalc` and `LoopTools`. A. T. would like to thank the International Centre for Theoretical Physics - South American Institute for Fundamental Research (ICTP-SIAFR) and the Istituto de Fisica Teorica at the Sao Paulo State University (IFT-UNESP) for hospitality.

APPENDIX: RELATION WITH EFT

Let us consider the operator $\mathcal{O}_1$ that we introduced in Eq. (1):

$$\mathcal{O}_1 = \bar{t}\gamma^\mu T_A t D^\nu G^A_{\mu\nu}. \tag{A1}$$

It is possible to rewrite it as a specific combination of four-fermion operators belonging to the Warsaw basis [19]. In order to do that we perform an appropriate field redefinition by using the gluon equations of motion

$$D^\nu G^A_{\mu\nu} = -g_s \sum_q \bar{q}\,\gamma^\mu T^A q, \tag{A2}$$

where $\sum_q$ denotes the sum over all quarks. In this case we have

$$\mathcal{O}_1 = -g_s \bar{t}\gamma^\mu T_A t \sum_q \bar{q}\,\gamma^\mu T^A q \tag{A3}$$

$$= -g_s \bar{t}\gamma^\mu T_A t(\bar{u}\gamma^\mu T^A u + \bar{d}\gamma^\mu T^A d + \cdots) \tag{A4}$$

where the ellipsis denotes second- and third-generation quark currents. The relevant combination that enters in $t\bar{t}$ production at the LHC and Tevatron is the one that couples the top-quark current with the up- and down-quark current, namely

$$\bar{t}\gamma^\mu T_A t(\bar{u}\gamma^\mu T^A u + \bar{d}\gamma^\mu T^A d). \tag{A5}$$

The following four-fermion operators of the Warsaw basis [19] are those relevant for $t\bar{t}$ production induced by the partonic subprocesses $u\bar{u}$, $d\bar{d} \to t\bar{t}$

$$
\begin{aligned}
\mathcal{O}_{qq}^{(1)1331} &= (\bar{u}_L\gamma_\mu t_L)(\bar{t}_L\gamma^\mu u_L) + \cdots \\
\mathcal{O}_{uu}^{1331} &= (\bar{u}_R\gamma_\mu t_R)(\bar{t}_R\gamma^\mu u_R) \\
\mathcal{O}_{qq}^{(1)1133} &= (\bar{u}_L\gamma_\mu u_L)(\bar{t}_L\gamma^\mu t_L) \\
&\quad + (\bar{d}_L\gamma_\mu d_L)(\bar{t}_L\gamma^\mu t_L) + \cdots \\
\mathcal{O}_{qq}^{(3)1133} &= (\bar{u}_L\gamma_\mu u_L)(\bar{t}_L\gamma^\mu t_L) \\
&\quad - (\bar{d}_L\gamma_\mu d_L)(\bar{t}_L\gamma^\mu t_L) + \cdots \\
\mathcal{O}_{uu}^{1133} &= (\bar{u}_R\gamma_\mu u_R)(\bar{t}_R\gamma^\mu t_R) \\
\mathcal{O}_{qu}^{(8)1133} &= (\bar{u}_L\gamma_\mu T^A u_L)(\bar{t}_R\gamma^\mu T^A t_R) \\
&\quad + (\bar{d}_L\gamma_\mu T^A d_L)(\bar{t}_R\gamma^\mu T^A t_R) \\
\mathcal{O}_{qu}^{(8)3311} &= (\bar{t}_L\gamma_\mu T^A t_L)(\bar{u}_R\gamma^\mu T^A u_R) + \cdots \\
\mathcal{O}_{qq}^{(3)1331} &= (\bar{u}_L\gamma_\mu t_L)(\bar{t}_L\gamma^\mu u_L) \\
&\quad + 2(\bar{d}_L\gamma_\mu t_L)(\bar{t}_L\gamma^\mu d_L) + \cdots \\
\mathcal{O}_{ud}^{(8)3311} &= (\bar{t}_R\gamma_\mu T^A t_R)(\bar{d}_R\gamma^\mu T^A d_R) \\
\mathcal{O}_{qd}^{(8)3311} &= (\bar{t}_L\gamma_\mu T^A t_L)(\bar{d}_R\gamma^\mu T^A d_R) + \cdots
\end{aligned}
\tag{A6}
$$

where the ellipses denote terms that do not contain two top quarks and two up quarks or two top quarks and two down quarks. In deriving some of the expressions in Eq. (A6) we made use of the Pauli matrices' completeness relation

$$
\sigma^I_{ij}\sigma^I_{kl} = 2\delta_{il}\delta_{jk} - \delta_{ij}\delta_{kl}. \tag{A7}
$$

By using the $SU(3)$ generators' completeness relation

$$
T^A_{ab}T^A_{cd} = \frac{1}{2}\delta_{ad}\delta_{bc} - \frac{1}{6}\delta_{ab}\delta_{cd} \tag{A8}
$$

and the Fierz rearrangement for anticommuting spinors

$$
\bar{\psi}_{1L}\gamma_\mu\psi_{2L}\bar{\psi}_{3L}\gamma^\mu\psi_{4L} = \bar{\psi}_{1L}\gamma_\mu\psi_{4L}\bar{\psi}_{3L}\gamma^\mu\psi_{2L} \tag{A9}
$$

$$
\bar{\psi}_{1R}\gamma_\mu\psi_{2R}\bar{\psi}_{3R}\gamma^\mu\psi_{4R} = \bar{\psi}_{1R}\gamma_\mu\psi_{4R}\bar{\psi}_{3R}\gamma^\mu\psi_{2R}, \tag{A10}
$$

the operator $\mathcal{O}_1$ can be rewritten in terms of the following specific combination of four-fermion operators:

$$
\begin{aligned}
\bar{t}\gamma^\mu T_A t D^\nu G^A_{\mu\nu} = {} & \frac{1}{4}\mathcal{O}_{qq}^{(1)1331} - \frac{1}{6}\mathcal{O}_{qq}^{(1)1133} \\
& + \frac{1}{2}\mathcal{O}_{uu}^{1331} - \frac{1}{6}\mathcal{O}_{uu}^{1133} \\
& + \mathcal{O}_{qu}^{(8)1133} + \mathcal{O}_{qu}^{(8)3311} \\
& + \frac{1}{4}\mathcal{O}_{qq}^{(3)1331} + \mathcal{O}_{ud}^{(8)3311} \\
& + \mathcal{O}_{qd}^{(8)3311}.
\end{aligned}
$$

This operator equivalence holds when considering $t\bar{t}$ production induced by the partonic subprocesses $u\bar{u}$, $d\bar{d} \to t\bar{t}$. The operator $\mathcal{O}_{qq}^{(3)1133}$ does not enter in the linear combination of Eq. (A11), and therefore any new physics that generates it is not captured by the operator $\mathcal{O}_1$.

More in general, in the EFT approach, the operators in Eq. (A6) enter in the $t\bar{t}$ production cross section induced by $u\bar{u}$, $d\bar{d}$ in the initial state through four specific linear combinations of their coefficients [9,16], namely

$$
\begin{aligned}
C_u^1 &= 6C_{qq}^{(1)1331} + 3C_{uu}^{1331} \\
&\quad - C_{qq}^{(1)1133} - C_{qq}^{(3)1133} - C_{uu}^{1133} \\
C_u^2 &= -C_{qu}^{(8)1133} - C_{qu}^{(8)3311} \\
C_d^1 &= 3C_{qq}^{(3)1331} - 3C_{qq}^{(1)1331} \\
&\quad + C_{qq}^{(3)1133} - C_{qq}^{(1)1133} + 6C_{ud}^{(8)3311} \\
C_d^2 &= -C_{qu}^{(8)1133} - C_{qd}^{(8)3311}.
\end{aligned}
\tag{A11}
$$

In case of $\mathcal{O}_1$ we have a unique coefficient and therefore the two approaches are not equivalent.

[1] B. Grzadkowski, Z. Hioki, K. Ohkuma, and J. Wudka, Probing anomalous top quark couplings induced by dimension-six operators at photon colliders, Nucl. Phys. **B689**, 108 (2004).

[2] B. Lillie, J. Shu, and T. M. P. Tait, Top compositeness at the Tevatron and LHC, J. High Energy Phys. 04 (2008) 087.

[3] D. Choudhury and P. Saha, Probing top anomalous couplings at the Tevatron and the Large Hadron Collider, Pramana **77**, 1079 (2011).

[4] Z. Hioki and K. Ohkuma, Latest constraint on nonstandard top-gluon couplings at hadron colliders and its future prospect, Phys. Rev. D **88**, 017503 (2013).

[5] J. F. Kamenik, M. Papucci, and A. Weiler, Constraining the dipole moments of the top quark, Phys. Rev. D **85**, 071501 (2012); Erratum, Phys. Rev. D **88**, 039903(E) (2013).

[6] S. S. Biswal, S. D. Rindani, and P. Sharma, Probing chromomagnetic and chromoelectric couplings of the top quark using its polarization in pair production at hadron colliders, Phys. Rev. D **88**, 074018 (2013).

[7] S. D. Rindani, P. Sharma, and A. W. Thomas, Polarization of top quark as a probe of its chromomagnetic and chromoelectric couplings in tW production at the Large Hadron Collider, J. High Energy Phys. 10 (2015) 180.

[8] K. Kumar, T. M. P. Tait, and R. Vega-Morales, Manifestations of top compositeness at colliders, J. High Energy Phys. 05 (2009) 022.
[9] C. Zhang and S. Willenbrock, Effective-field-theory approach to top-quark production and decay, Phys. Rev. D **83**, 034006 (2011).
[10] C. Zhang, N. Greiner, and S. Willenbrock, Constraints on non-standard top quark couplings, Phys. Rev. D **86**, 014024 (2012).
[11] C. Degrande, J. M. Gerard, C. Grojean, F. Maltoni, and G. Servant, Non-resonant new physics in top pair production at hadron colliders, J. High Energy Phys. 03 (2011) 125.
[12] C. Englert, A. Freitas, M. Spira, and P. M. Zerwas, Constraining the intrinsic structure of top-quarks, Phys. Lett. B **721**, 261 (2013).
[13] C. Degrande, J. M. Gerard, C. Grojean, F. Maltoni, and G. Servant, Probing top-Higgs non-standard interactions at the LHC, J. High Energy Phys. 07 (2012) 036; Erratum, J. High Energy Phys. 03 (2013) 32.
[14] V. Cirigliano, W. Dekens, J. de Vries, and E. Mereghetti, Constraining the top-Higgs sector of the standard model effective field theory, Phys. Rev. D **94**, 034031 (2016).
[15] C. Englert, L. Moore, K. Nordstrom, and M. Russell, Giving top quark effective operators a boost, Phys. Lett. B **763**, 9 (2016).
[16] A. Buckley, C. Englert, J. Ferrando, D. J. Miller, L. Moore, M. Russell, and C. D. White, Global fit of top quark effective theory to data, Phys. Rev. D **92**, 091501 (2015); Constraining top quark effective theory in the LHC Run II era, J. High Energy Phys. 04 (2016) 015.
[17] C. Englert, R. Kogler, H. Schulz, and M. Spannowsky, Higgs coupling measurements at the LHC, Eur. Phys. J. C **76**, 393 (2016).
[18] M. Fabbrichesi, M. Pinamonti, and A. Tonero, Stringent limits on top-quark compositeness from $t\bar{t}$ production at the Tevatron and the LHC, Phys. Rev. D **89**, 074028 (2014).
[19] B. Grzadkowski, M. Iskrzynski, M. Misiak, and J. Rosiek, Dimension-six terms in the Standard Model Lagrangian, J. High Energy Phys. 10 (2010) 085.
[20] D. B. Franzosi and C. Zhang, Probing the top-quark chromomagnetic dipole moment at next-to-leading order in QCD, Phys. Rev. D **91**, 114010 (2015).
[21] R. Contino, A. Falkowski, F. Goertz, C. Grojean, and F. Riva, On the validity of the effective field theory approach to SM precision tests, J. High Energy Phys. 07 (2016) 144.
[22] C. Degrande, C. Duhr, B. Fuks, D. Grellscheid, O. Mattelaer, and T. Reiter, UFO—The universal FeynRules output, Comput. Phys. Commun. **183**, 1201 (2012).
[23] A. Alloul, N. D. Christensen, C. Degrande, C. Duhr, and B. Fuks, FeynRules 2.0—A complete toolbox for tree-level phenomenology, Comput. Phys. Commun. **185**, 2250 (2014).
[24] J. Alwall, R. Frederix, S. Frixione, V. Hirschi, F. Maltoni, O. Mattelaer, H.-S. Shao, T. Stelzer, P. Torrielli, and M. Zaro, The automated computation of tree-level and next-to-leading order differential cross sections, and their matching to parton shower simulations, J. High Energy Phys. 07 (2014) 079.
[25] E. Conte, B. Fuks, and G. Serret, MadAnalysis 5, A user-friendly framework for collider phenomenology, Comput. Phys. Commun. **184**, 222 (2013).
[26] A. M. Sirunyan *et al.* (CMS Collaboration), Measurement of the $t\bar{t}$ production cross section using events with one lepton and at least one jet in pp collisions at $\sqrt{s} = 13$ TeV, J. High Energy Phys. 09 (2017) 051.
[27] V. Khachatryan *et al.* (CMS Collaboration), Measurement of the t-tbar production cross section in the e-mu channel in proton-proton collisions at sqrt(s) = 7 and 8 TeV, J. High Energy Phys. 08 (2016) 029.
[28] F. P. Schilling (ATLAS, CDF, CMS, and D0 Collaborations), Measurements of the top quark pair-production cross section, Eur. Phys. J. Web Conf. **49**, 04001 (2013).
[29] J. A. Aguilar-Saavedra, B. Fuks, and M. L. Mangano, Pinning down top dipole moments with ultra-boosted tops, Phys. Rev. D **91**, 094021 (2015).
[30] T. Aaltonen *et al.* (CDF Collaboration), First Measurement of the t Anti-t Differential Cross Section d Sigma/dM(t Anti-t) in p Anti-p Collisions at s ∗ ∗(1/2) = 1.96-TeV, Phys. Rev. Lett. **102**, 222003 (2009).
[31] V. M. Abazov *et al.* (D0 Collaboration), Measurement of differential $t\bar{t}$ production cross sections in $p\bar{p}$ collisions, Phys. Rev. D **90**, 092006 (2014).
[32] CMS Collaboration, Report No. CMS-PAS-TOP-16-013.
[33] CMS Collaboration, Report No. CMS-PAS-TOP-16-007.
[34] ATLAS Collaboration, Report No. ATLAS-CONF-2016-040.
[35] ATLAS CollaborationReport No. ATLAS-CONF-2016-100.
[36] M. Aaboud *et al.* (ATLAS Collaboration), Measurements of top-quark pair differential cross-sections in the $e\mu$ channel in pp collisions at $\sqrt{s} = 13$ TeV using the ATLAS detector, Eur. Phys. J. C **77**, 299 (2017).
[37] Y. T. Chien, V. Cirigliano, W. Dekens, J. de Vries, and E. Mereghetti, Direct and indirect constraints on CP-violating Higgs-quark and Higgs-gluon interactions, J. High Energy Phys. 02 (2016) 011.
[38] H. H. Patel, Package-X: A Mathematica package for the analytic calculation of one-loop integrals, Comput. Phys. Commun. **197**, 276 (2015); Package-X 2.0: A Mathematica package for the analytic calculation of one-loop integrals, Comput. Phys. Commun. **218**, 66 (2017).
[39] B. C. Nejad, J.-N. Lang, T. Hahn, and E. Mirabella, FormCalc 8: Better algebra and vectorization, Acta Phys. Pol. B **44**, 2231 (2013).
[40] ATLAS and CMS Collaborations, Report No. ATLAS-CONF-2015-044.
[41] CMS Collaboration, Report No. CMS-NOTE-2012-006.